Cycle-basis-informed Heuristic Method for Radial Distribution System Reconfiguration

Anton Hinneck, Mathias Duckheim, Michael Metzger, and Stefan Niessen

***Abstract*—Distribution system reconfiguration (DSR) uses switching actions, which are available to distribution system operators (DSOs) without regulatory changes, to optimize the grid topology. Although distribution systems often support meshed operation, they are typically operated radially to simplify fault isolation and improve reliability. The minimization of active power losses not only improves efficiency but also helps prevent voltage and current limit violations. However, the DSR problem is computationally difficult due to its combinatorial and non-convex nature. This paper proposes a cycle-basis-informed heuristic method for radial DSR, aiming to reduce active power losses and stabilize the voltage. The proposed heuristic method works directly with the non-convex AC load flow model, considering switching actions as the only degrees of freedom. A large neighborhood search framework is used, constructing restricted mixed-integer nonlinear programming (MINLP) subproblems of controllable complexity. Radiality is ensured via a graph-theoretic method based on the cycle basis of the system, enabling systematic exploration of feasible configurations. The proposed heuristic method is evaluated on benchmark systems with varying load profiles, demonstrating robust performance, effective loss reduction, improved voltage profiles, and practical computation time. These results confirm its applicability to real-world DSR in radial AC systems.**

***Index Terms*—Distribution system reconfiguration, reliability, mixed-integer nonlinear programming (MINLP), topology optimization, large neighborhood search, cycle basis, radial AC system.**

NOMENCLATURE

$\mathcal{N}$	A graph/power system topology
$\alpha(\mathcal{N})$	Number of cycle edges in $\mathcal{N}$
$\beta(\mathcal{N})$	Cyclomatic number of $\mathcal{N}$
ψ	Number of switchable lines in heuristic method
τ^H	Number of spanning trees for heuristic distribution system reconfiguration (H-DSR)
τ^C	Number of spanning trees for complete distribution system reconfiguration (C-DSR)
$\Delta\theta_{ft}$	Voltage angle difference between buses f and t
Δp^L	Loss reduction
θ_f, θ_t	Voltage angle at buses f and t
$\underline{\rho}^*$	Lower bound of objective value
ρ	Objective value
γ^v, γ^s	Absolute violations of voltage and power limits
$\mathcal{E}^{\mathcal{S}}$	Set of switchable lines and edges
$\mathcal{E}^U$	Unique edge set (UES)
$\mathcal{E}^{U,\psi}$	Reduced unique edge set (rUES)
$\mathcal{E}_k^{\mathcal{N}}$	UES in the k^{th} cycle in $\mathcal{E}^{\mathcal{N}}$
$\mathcal{B}$	A cycle basis of $\mathcal{N}$
$\mathcal{C}^{\mathcal{N}}$	Set of all cycles in $\mathcal{N}$
$\mathcal{C}_k^{\mathcal{N}}$	The k^{th} cycle in $\mathcal{C}^{\mathcal{N}}$
$\mathcal{C}_k^{\mathcal{B}}$	The k^{th} fundamental cycle in $\mathcal{B}$
$c(\mathcal{N})$	Number of disconnected components in $\mathcal{N}$
ct	Computation time
g_{ft}^{sh}, b_{ft}^{sh}	Shunt conductance and susceptance of line ft
g_{ft}, b_{ft}	Conductance and susceptance of line ft
$g, \mathcal{G}_f$	Index and set of generators at bus f
$\mathcal{H}$	A (spanning) subgraph in $\mathcal{N}$
I_{ft}	Current through line ft
$l, \mathcal{L}_f$	Index and set of loads at bus f
p_g^G, q_g^G	Real and reactive power injections of source g
p_{ft}, q_{ft}	Real and reactive power flows from buses f to t
p_l, q_l	Real and reactive power draws of load l
p^L	Absolute power loss
$\bar{s}_{ft}$, $\bar{\bar{s}}_{ft}$	Power ratings 1 and 2 of line ft
$\mathcal{T}$	A spanning tree in $\mathcal{N}$
$\bar{\mathcal{T}}$	A co-tree of $\mathcal{T}$ in $\mathcal{N}$
$v_f^{m,ref}$	Measured voltage magnitude at reference bus f
v^{base}	Base voltage of test system
V_f^m, V_t^m	Voltage magnitudes at buses f and t
$\mathcal{V}^{ref}$	Set of reference buses/vertices

Manuscript received: November 28, 2024; revised: April 9, 2025; accepted: June 17, 2025. Date of CrossCheck: June 17, 2025. Date of online publication: July 15, 2025.

A. Hinneck (corresponding author) is with the Faculty of Electrical Engineering and Information Technology, Technical University of Darmstadt, Darmstadt, Germany, and he is also with the Distribution System Operator Stromnetz, Berlin, Germany (e-mail: anton.hinneck@stromnetz-berlin.de).

M. Duckheim is with Siemens AG, Foundational Technologies, Erlangen, Germany (e-mail: mathias.duckheim@siemens.com).

M. Metzger is with Siemens AG, Foundational Technologies, Munich, Germany, and he is also with the School of Engineering and Design, Technical University of Munich, Munich, Germany (e-mail: michael.metzger@siemens.com).

S. Niessen is with the Faculty of Electrical Engineering and Information Technology, Technical University of Darmstadt, Darmstadt, Germany, and he is also with Siemens AG, Foundational Technologies, Erlangen, Germany (e-mail: stefan.niessen@siemens.com).

DOI: 10.35833/MPCE.2024.001212

$\underline{V}_f^m$, $\overline{V}_f^m$ The minimum and maximum voltage magnitudes at bus f

y_{ft}, r_{ft} Admittance and resistance of line ft

z_{ft} Switching status of line ft

I. Introduction

USING switching actions to reduce losses and improve operation conditions has received continued attention for decades [1]. Switching actions are identified as an effective mechanism for controlling electrical networks to achieve a multitude of objectives such as influencing short-circuit currents and removing overloads [2], [3]. Moreover, voltage profiles can be improved and voltage band violations can be prevented [4]. The European Smart Grid Strategy [5] identifies the development of tools that enable rapid integration of distributed energy resources while maintaining operation limits as a key objective. To that end, support for bidirectional power flows (PFs) in distribution systems is strictly required. In addition to feasible operation conditions, topological requirements must be met, as distribution systems are commonly operated as radial systems. Meshed operation of power systems generally results in lower power losses and balanced use of the equipment, which is only an advantage if all equipment in a path is rated for similar operation conditions, and better voltage profiles. Meshed systems are more expensive to plan and operate because higher short-circuit currents must be taken into account, and more elaborate protection schemes are required. Radial system protection is less expensive and widely adopted with open-loop designs that provide sufficient supply security [6]. Detecting fault locations is also easier. In addition to technical aspects, economic aspects are also a factor. Although a system operator in Germany is allowed to collect costs for system power losses through system fees from their customers, so far no incentive structure exists to minimize them. However, increases in efficiency have become the focus of policy makers. National and European level policies such as the Green Deal have redefined requirements for energy infrastructure, which especially affect distribution system operators (DSOs). In a recent publication [7], challenges for DSOs are summarized. First, a new infrastructure for alternative fuels must be developed for electric vehicle (EV), which requires significant investments in distribution systems. Prior to the deployment of EV charging points, the readiness of the system must be assessed. Important factors are residual capacity and contributions to operation flexibility. With regard to housing, the process of installing heat pumps and renewable energy source (RES) installations must become more efficient. These measures alone demonstrate the need for system fortification to support the increasing number of domestic charging stations, heat pumps, and rooftop solar infeed. This fortification is also required for the secondary system. More electric power transported via the distribution system generally means increasing efforts for planning, operation, and larger potentials for optimization. With regard to energy losses, a new European directive on energy efficiency targets a decrease in energy consumption by 11.7% by 2030, which is to be achieved by increases in efficiency. Network losses are a significant factor as defined in Article 25 (3) 2021/0203 in [8]: "Member states shall ensure that transmission and distribution system operators monitor and quantify the overall volume of network losses and, where it is technically and financially feasible, optimize networks, and improve network efficiency. Transmission and distribution system operators shall report these measures and expected energy savings through the reduction of network losses to the national energy regulatory authority." Costs for loss energy can reach between 20 and 100 million euros per year for a city like Berlin, Germany, depending on the wholesale energy prices [9].

DSOs in Germany commonly operates high voltage (HV) and medium voltage (MV) systems. Three topological structures are used mainly to operate MV systems, open and closed rings, as well as radial feeds, according to the national standard VDE-AR-N 4110 [10] or amendments by German DSOs, e. g., [11]. The radial and open-ring structures are similar with the major difference that the open ring generally allows for fast re-energization of customers after a fault has been located, thereby increasing the supply security. The closed ring is used to connect customers that require a high security of supply but has the major disadvantage that it requires more advanced and costly protection systems and equipment. According to VDE-AR-N 4110, which sets the standard for MV systems in Germany operating at nominal voltages between 1 kV and 60 kV, a tolerable voltage band of ±10% relative to the system base voltage is required during normal grid operation [10]. DSOs commonly amend the standard due to the particularities in their area of operation. Therefore, they may adjust the admissible voltage band. In the US, the ANSI C84.1 [12] defines acceptable voltages from approximately ±5% to ±10% depending on the equipment and its application.

In [13], methods for distribution system reconfiguration (DSR) are classified and assigned to one of three categories: optimization-based heuristics, heuristics, and machine learning methods. Heuristics and machine learning methods have been shown to find good solutions for DSR but are not considered in this paper. This paper focuses on optimization models, which have the advantage of theoretical guarantees that are not necessarily available with other methods. Moreover, deterministic algorithms are readily available, ensuring reproducibility. Competing heuristic methods like simulated annealing, genetic methods, and other biology-inspired methods may rely on stochastic methods that suffer from poor reproducibility, limiting continuous improvement in a software product. Deterministic heuristic methods such as tabu or greedy searches offer few or no theoretical guarantees, but they can often achieve good objective improvements quickly for certain problem instances. The major drawback of machine learning methods is their black-box nature, which is specifically true for deep neural networks. Although such methods can be effective, the trained model and results may not behave entirely predictably. As power systems are highly regulated and a matter of national security, transparent decision-making is key and cannot be guaranteed for many methods, but it is currently considered in the research [14].

In this paper, topologies are optimized to minimize active power losses. The topology of an electrical network can be represented by a graph $\mathcal{N}=\{\mathcal{V},\mathcal{E}\}$, where $\mathcal{V}$ denotes a set of vertices and $\mathcal{E}$ denotes a set of edges [15]. Every edge is a tuple of a start bus f and a termination bus t, denoted as line ft in the following. In an electrical network, every vertex is assigned to a bus and every edge is assigned to a conductor of energy such as a power line, transformer, or other equipment. Topologies in power systems must often meet qualitative criteria. Most importantly, a power system is radial if the graph representing its topology is a spanning tree (ST). Modeling the electrical state of a power system requires PF expressions and integer variables to consider the opening and closing of switches in the respective optimization models. PF equations are non-convex, which makes them difficult to solve or comes at the cost of theoretical guarantees. The same applies to integrality constraints on variables. Although there are specialized mixed-integer nonlinear programming (MINLP) solvers, the resulting problems are often not tractable due to their complexity for real-world applications. Many optimization models for DSR have been proposed. These entail mixed-integer linear programs (MILPs) [16]-[24] that relax power flow (PF) constraints to linear expressions. Removing integrality, one obtains a convex problem that has significant computational advantages. Approximations may also yield mixed-integer quadratic programs (MIQPs) and mixed-integer second-order cone programs (MISOCs) [25] - [33]. Especially, the second-order cone (SOC) approximation has interesting properties, as it is exact for radial systems if nodal power injections and line flows are unbounded from below [15]. Lastly, general MINLPs do not provide general guarantees for global optimality but are the most accurate and versatile in solving AC load flow problems with discrete decisions [34]-[39], and the primary drawback lies in the computational burden.

Several methods have been proposed to ensure radiality of topologies. First, the so-called parent-child formulation is commonly used, which ensures that every vertex has only a single parent vertex, excluding the root vertex [16], [18], [20], [22], [28], [29], [40]. $2|\mathcal{E}|$ more (often integer-valued) variables are required, which leads to a significantly more complex model. If no integer variables are used, the parent-child formulation suffers from the same issues as the connectivity-based ST definition. Thus, it is not considered as a benchmark in this paper. The first ST definition used as a benchmark is based on the connectivity-based ST definition in Supplementary Material A. This formulation is used in [19], [23], [25]-[27], [30]-[32], [37], [38] with shortcomings discussed in [37]. Especially, zero-injection nodes and distributed generation can lead to islanding and formation of cycles. The acyclicity-based ST definition, based on Supplementary Material A, is also used as a benchmark [19], [21], [24], [39] but can lead to very complex formulations, as enumerating all cycles can lead to a massive constraint set and can take well over a day (as shown for synthetic test cases in [41]) before a model can even be built and solved.

For the reader's convenience, the models in the following are always denoted along with their equation numbers at the point of definition in subscript. The literature review shows that only few DSR models use exact AC PF constraints. Of these, none discuss mixed-integer programming (MIP) heuristic methods. MIP heuristic methods play a vital role in providing first improvements quickly, where more complex formulations may require significant computation time, at the cost of potentially eliminating good solutions from the search space. In this paper, we propose a cycle-basis-informed heuristic method for radial distribution system reconfiguration. The contributions in this paper are threefold:

1) We present a theoretical result ensuring the radiality of distribution system topologies.

2) We devise an MINLP heuristic method based on the result for radial AC PF called heuristic DSR, i.e., H-DSR$_{(13)}$, supporting distributed generation and zero-injection nodes, which does not require the full set of cycles.

3) We conduct an in-depth comparison against relaxed radiality DSR, i.e., RR-DSR$_{(11)}$, which is a reference model that uses the connectivity-based ST definition [37], [38] and complete DSR, i.e., C-DSR$_{(12)}$ [39], using acyclicity.

II. PREREQUISITES

A. Large Neighborhood Search (LNS)

Different types of heuristic methods exist in the field of optimization. A commonly applied and generally applicable method is called LNS, which is an MIP heuristic method. MIP heuristic method constructs a new MIP of reduced complexity. A respective method was introduced in [42] for MILP with an application to MINLP discussed in [43]. Applying this general methodology to an AC PF problem [44] including line switching results in restrictable DSR, i.e., R-DSR$_{(1)}$, to be introduced in the next section. Implementing LNS, we enforce $z_{ft}=1$, if a switch is excluded from the search space.

B. R-DSR

The basis for the models presented in this paper is provided as R-DSR$_{(1)}$ in (1), similar to [45]. The model allows for applying LNS to DSR. Like in [45], a PF formulation is at the core of this model, which is based on [44] and can be derived from the π-model of a transmission line [46]. It is applicable to single-phase or symmetric three-phase systems.

$$\min_{V^m,\theta,p^G,q^G,p,q} \rho \sum_{g\in\mathcal{G}} p_g^G \tag{1a}$$

$$\sum_{g\in\mathcal{G}_f} p_g^G = \sum_{t\in\mathcal{E}_f} p_{ft} + \sum_{t\in\mathcal{E}_f} p_{tf} + \sum_{l\in\mathcal{L}_f} p_l \quad \forall f\in\mathcal{V} \tag{1b}$$

$$\sum_{g\in\mathcal{G}_f} q_g^G = \sum_{t\in\mathcal{E}_f} q_{ft} + \sum_{t\in\mathcal{E}_f} q_{tf} + \sum_{l\in\mathcal{L}_f} q_l \quad \forall f\in\mathcal{V} \tag{1c}$$

$$p_{ft}=[(V_f^m)^2(g_{ft}+g_{ft}^{sh}) - V_f^m V_t^m g_{ft}\cos(\Delta\theta_{ft}) - V_f^m V_t^m b_{ft}\sin(\Delta\theta_{ft})]z_{ft} \quad \forall ft, tf\in\mathcal{E}^{\mathcal{S}} \tag{1d}$$

$$q_{ft} = -[(V_f^m)^2 (b_{ft} + b_{ft}^{sh}) + V_f^m V_t^m b_{ft} \cos(\Delta\theta_{ft}) - V_f^m V_t^m g_{ft} \sin(\Delta\theta_{ft})] z_{ft} \quad \forall ft, tf \in \mathcal{E}^{\mathcal{S}} \tag{1e}$$

$$p_{ft} = (V_f^m)^2 (g_{ft} + g_{ft}^{sh}) - V_f^m V_t^m g_{ft} \cos(\Delta\theta_{ft}) - V_f^m V_t^m b_{ft} \sin(\Delta\theta_{ft}) \quad \forall ft, tf \in \mathcal{E}^{\mathcal{A}} \tag{1f}$$

$$q_{ft} = -(V_f^m)^2 (b_{ft} + b_{ft}^{sh}) + V_f^m V_t^m b_{ft} \cos(\Delta\theta_{ft}) - V_f^m V_t^m g_{ft} \sin(\Delta\theta_{ft}) \quad \forall ft, tf \in \mathcal{E}^{\mathcal{A}} \tag{1g}$$

$$V_f^m = v_f^{m,ref} \quad \forall f \in \mathcal{V}^{ref} \tag{1h}$$

In all models, consumers in $\mathcal{L}$ are modeled using the passive sign convention. Power sources in $\mathcal{G}$, which are connections to an external grid in this paper, are modeled using the active sign convention. Hence, in RES-dominated instances, the net power injection of prosumers and the power injected into the feeder are negative if more power is produced than consumed. The sign conventions are considered in the active (1b) and reactive (1c) power balances. Next, a known voltage is set at a reference bus that is usually located at the substation by constraint (1h). Last, the PF into branches is modeled by (1d)-(1g). To improve readability, we define $\Delta\theta_{ft}{:}\theta_f - \theta_t$. Here, these equalities only apply to $ft \in \mathcal{E} \backslash \mathcal{E}^{\mathcal{S}}$ (when ft is not switchable), or if $z_{ft} = 1$ (when ft is operational). To ensure brevity, we define $\mathcal{E}^{\mathcal{A}} := \mathcal{E} \backslash \mathcal{E}^{\mathcal{S}}$, with $\mathcal{E}^{\mathcal{A}}$ denoting a set of switches excluded from the search space. Otherwise, it holds that $p_{ft} = q_{ft} = p_{tf} = q_{tf} = z_{ft} = 0$. The power injected into a feeder is minimized by objective function (1a).

1) Safety Ratings

A main requirement in practice is to maintain safe voltage and power levels to prevent equipment damage and personnel risk.

$$\underline{V}_f^m \leq V_f^m \leq \overline{V}_f^m \quad \forall f \in \mathcal{V} \tag{2}$$

$$p_{ft}^2 + q_{ft}^2 \leq \bar{s}_{ft}^2 \quad \forall ft \in \mathcal{E} \tag{3}$$

The optimization problems in this paper are relaxed by removing (2) and (3) from constraint sets of MINLP and evaluating their violation after optimization terminates. This is to illustrate the main contribution, which is the heuristic method for reconfiguration. These constraints, especially (2), are commonly active and would render many solutions infeasible, especially those found on small domains and early during optimization. Relaxing these constraints has practical merits because the resulting methods can produce improved states even if the system is at risk and no nominal operational states exist. Furthermore, the objective function (1a) minimizes power loss, which includes squared current flows. Minimizing this term incentivizes balanced equipment utilization and adherence to constraints (2) and (3) as a form of soft constraint. As constraint violations may be tolerated, detection and tracking are essential for operators to make informed decisions. Therefore, this is an integral step in our post-processing, as documented later in this paper that reports computational results. To make documentation concise, γ^v and γ^s are defined in (4) and (5). The values of γ are 0, if the respective constraint is not violated. Otherwise, the values of γ are equal to the violations of the constraint. The values of γ_f^v are used to detect and track violations of 2 sets of constraints, and only the maximum violation is saved for each constraint tuple because only one expression $\underline{V}_f^m - V_f^m < 0$ or $V_f^m - \overline{V}_f^m < 0$ can be true at any given time for an element $f \in \mathcal{V}$, if $\underline{V}_f^m \leq \overline{V}_f^m$.

$$\gamma_f^v := \begin{cases} 0 & (2) \text{ is satisfied} \\ \max(\underline{V}_f^m - V_f^m, V_f^m - \overline{V}_f^m) & \text{otherwise} \end{cases} \tag{4}$$

$$\gamma_{ft}^s := \begin{cases} 0 & (3) \text{ is satisfied} \\ (p_{ft}^2 + q_{ft}^2) - \bar{s}_{ft}^2 & \text{otherwise} \end{cases} \tag{5}$$

2) Losses and a Non-trivial Lower Bound on Power Injection

The objective of this paper is to minimize power losses. Thus, absolute power losses $p^L (\geq 0)$ must first be defined. This can be done according to the constraint (1b). Summing the active power balance over all buses in the network yields:

$$0 = \sum_{f \in \mathcal{V}} \left(\sum_{t \in \mathcal{E}_f} p_{ft} + \sum_{t \in \mathcal{E}_f} p_{tf} + \sum_{l \in \mathcal{L}_f} p_l - \sum_{g \in \mathcal{G}_f} p_g^G \right) \tag{6}$$

$$p^L := \sum_{f \in \mathcal{V}} \left(\sum_{t \in \mathcal{E}_f} p_{ft} + \sum_{t \in \mathcal{E}_f} p_{tf} \right) \tag{7}$$

Equation (6) shows four major terms: power flowing into and out of buses, generation at buses, and load at buses. The loads p_l are parameters in the model discussed. The PFs between buses are sources of power losses. Power losses that occur when current flows through a conductor of line ft can also be determined as $p_{ft}^L = z_{ft} r_{ft} I_{ft}^2$. If a line is out of operation, i.e., $z_{ft} = 0$, no current flows and power losses vanish. Hence, for system-wide p^L, one has $p^L = \sum_{ft \in \mathcal{E}} z_{ft} r_{ft} I_{ft}^2$. Substituting the expression for p^L in (6) yields:

$$\sum_{g \in \mathcal{G}} p_g^G = \sum_{ft \in \mathcal{E}} z_{ft} r_{ft} I_{ft}^2 + \underbrace{\sum_{l \in \mathcal{L}_f} p_l}_{\text{Constant}} \tag{8}$$

It can be observed that, as loads are constant, minimizing power injection as stated in (1a) means minimizing total system losses, which is a well-known result [15]. Injection power (i.e., generation power) is exactly the total power required for the system operation, so (6) and (1b) hold. By using (6) and (7), system-wide losses can also be expressed as:

$$p^L = \sum_{f \in \mathcal{V}} \sum_{g \in \mathcal{G}_f} p_g^G - \sum_{f \in \mathcal{V}} \sum_{l \in \mathcal{L}_f} p_l \tag{9}$$

The equality in (9) may also be employed to derive a non-trivial lower bound for (1a), which remains applicable to the models introduced subsequently. This is important as R-DSR$_{(1)}$ is non-convex, even when binary variables z_{ft} are neglected, since $\sin(x)$, $\cos(x)$, and products of variables like V_f^m, V_t^m are non-convex functions. Hence, there is no guarantee that either the original model or its modification, e.g., non-linear programming (NLP) relaxation computed by the solver [47] for deriving a lower bound, is solved for global optimality. With the lower bound in (10), the quality of solutions can be assessed. Rearranging (9), we have:

$$\sum_{f\in\mathcal{V}}\sum_{g\in\mathcal{G}_f} p_g^G = \min_{V^m,\theta,p^G,q^G,p,q} \rho \sum_{g\in\mathcal{G}} p_g^G = p^L + \sum_{f\in\mathcal{V}}\sum_{l\in\mathcal{L}_f} p_l \overset{p^L\geq 0}{\geq} \sum_{f\in\mathcal{V}}\sum_{l\in\mathcal{L}_f} p_l =: \rho_-^* \tag{10}$$

C. Reference Models

The first reference model introduced, as stated in (11), is referred to as RR-DSR$_{(11)}$, and is used in slightly altered form in previous research works [37], [38]. The radiality condition used in this model is presented in Supplementary Material A, i.e., the connectivity-based ST definition. This theorem and other related fundamentals can be found in Supplementary Material A, too.

$$\begin{cases} \text{(1a)-(1h)} \\ \mathcal{E}^S = \mathcal{E} \end{cases} \tag{11a}$$

$$\sum_{ft\in\mathcal{E}} z_{ft} = |\mathcal{V}| - 1 \tag{11b}$$

In addition to PF constraint (11a), the radiality constraint (11b) is added. This is only part of the requirement, as the graph must also be connected. A proof under which conditions power balance constraints (1b) and (1c) ensure connectedness can be found in [37]. This model is called relaxed radiality as constraint (11b) is not sufficient and radiality additionally relies on the structure of the DSR model and system data. A challenge for RR-DSR$_{(11)}$ poses so-called zero-injection nodes as these may be islanded and cycles may be formed. Zero-injection nodes may occur due to maintenance, behind-the-meter production (as an aid to model certain pieces of electrical equipment), as well as unplanned outages. Several methods are proposed to extend RR-DSR$_{(11)}$ to deal with these edge cases. First, an additional constraint may be added for every such node, requiring that at least one of the lines connected to it could be operational [26]. Second, if the injection of a node is zero, a small reactive power draw may be assigned that does not significantly alter the result [25]. A discussion of this particular issue can be found in [48]. Similar problems arise when multiple sources of electric power are connected, as is expected in RES-dominated systems with distributed generation.

The second reference model, which is called C-DSR$_{(12)}$ and presented in (12), enforces additional constraint (12b) and ensures acyclicity. This ensures that every cycle is at least missing one edge, whereby the resulting graph must be acyclic. To enumerate all cycles, Gibb's algorithm [49] is implemented.

$$\begin{cases} \text{(1a)-(1h)} \\ \mathcal{E}^S = \mathcal{E} \end{cases} \tag{12a}$$

$$\sum_{ft\in\mathcal{E}_k^{\mathcal{N}}} z_{ft} \leq |\mathcal{E}_k^{\mathcal{N}}| - 1 \quad \forall k\in\{1,2,\ldots,|\mathcal{C}^{\mathcal{N}}|\} \tag{12b}$$

$$\sum_{ft\in\mathcal{E}} z_{ft} = |\mathcal{V}| - 1 \tag{12c}$$

The radiality rests on the acyclicity-based definition of ST in Supplementary Material A. No requirements are imposed on the data of power system compared with the connectivity-based method. As shown in [39], $\mathcal{E}^S$ can be reduced for RR-DSR$_{(11)}$ and C-DSR$_{(12)}$ to $\mathcal{E}^S = \left\{ e\in\mathcal{E} \middle| e \in \bigcup_{\forall k} \mathcal{E}_k^{\mathcal{N}} \right\}$, where e is the edge (line) in the set $\mathcal{E}$, decreasing combinatorial complexity. Constraints (11b) and (12c) must then be replaced by $|\mathcal{E}| - |\mathcal{E}^S| + \sum_{ft\in\mathcal{E}^S} z_{ft} = |\mathcal{V}| - 1$.

III. Heuristic Method for DSR

In this paper, our aim is to derive a radial operational topology. The system structure is often meshed. However, when fully connected (all switches are closed), we assume that the system forms a simple graph. Deriving a radial operation topology then means finding a subgraph that is an ST. This section presents the theoretical foundation of the proposed heuristic method. Proofs of the presented results are deferred to Supplementary Material A. The main idea of the proposed heuristic method is to explore only a subset of all possible STs. To that end, we first require a method to determine STs. The proposed heuristic method defines a set of STs based on a CB of the system, which can then be restricted further to construct heuristic problem instances.

It is well known that given a simple cyclic graph $\mathcal{N}=(\mathcal{V},\mathcal{E})$, any ST $\mathcal{T}\subset\mathcal{N}$ defines a CB $\mathcal{B}$ through the set of edges that is not included in the ST, i.e., $\bar{\mathcal{T}}=\mathcal{E}\backslash\mathcal{T}$, where $\mathcal{T}$ is called the defining ST of $\mathcal{B}$, and $\bar{\mathcal{T}}$ is called the co-tree of $\mathcal{T}$. Each edge in $\bar{\mathcal{T}}$, when added to $\mathcal{T}$, completes a unique fundamental cycle (FC). The set of such created FC forms a CB. $\beta(\mathcal{N})$ states the number of elements in a CB. The first observation to be made is that the mapping from $\mathcal{B}$ to the defining ST $\mathcal{T}$ is generally not injective. In other words, multiple distinct STs may give rise to the same CB. The consequence of this is formalized in Lemma 1.

Lemma 1 Let $\mathcal{B}$ be a CB of $\mathcal{N}$. Then, any FC $\mathcal{C}_k^{\mathcal{B}}\in\mathcal{B}$ may contain more than one edge $ft\in\mathcal{E}(\mathcal{C}_k^{\mathcal{B}})$, which is not present in any other FC $\mathcal{C}_j^{\mathcal{B}}\in\mathcal{B}$, for $j\neq k$.

Based on this observation, we introduce the concept of unique edge sets (UESs), which contain one or more edges that are in a single FC of a CB, and others are defined in Definition 1.

Definition 1 (UES) Let $\mathcal{B}=\{\mathcal{C}_1^{\mathcal{B}},\mathcal{C}_2^{\mathcal{B}},\ldots,\mathcal{C}_{\beta(\mathcal{N})}^{\mathcal{B}}\}$ be a CB of $\mathcal{N}$. Define the UES $\mathcal{E}_k^U$ of an FC $\mathcal{C}_k^{\mathcal{B}}$ as $\mathcal{E}_k^U := \{ft\in\mathcal{E}(\mathcal{C}_k^{\mathcal{B}}) | ft\notin\mathcal{C}_j^{\mathcal{B}}, \forall j\neq k\}$.

In the following, we refer to the collection $\mathcal{E}^U=\{\mathcal{E}_1^U,\mathcal{E}_2^U,\ldots,\mathcal{E}_{\beta(\mathcal{N})}^U\}$ as UESs. Considering the construction of CB described earlier, Lemma 1 and Definition 1, an important observation must be noted. Each $\mathcal{E}_k^U$ must contain at least one element, i.e., $\left|\mathcal{E}_k^U\right|\geq 1$. This holds because an edge must be in the co-tree of the defining ST that gives rise to the respective FC $\mathcal{C}_k^{\mathcal{B}}$ initially. In addition, multiple edges unique to a single FC may exist according to Lemma 1. This leads to the following key result.

Theorem 1 Let $\mathcal{T}$ be the spanning subgraph formed by removing a single edge $ft\in\mathcal{E}_k^U$ from $\mathcal{N}$ for each $k=1,2,\ldots,\beta(\mathcal{N})$. Then, $\mathcal{T}$ is an ST.

Given a graph and forming $\mathcal{E}_k^U$ based on a CB, Theorem 1 allows us to easily identify STs. As our goal is to devise a heuristic method, this result can be used immediately to develop a simple ad-hoc heuristic method as follows.

1) *Step 1*: in model 1, close all switches by enforcing $z=1$.

2) *Step 2*: for every $\mathcal{E}_k^U$, select the first line $ft=\mathcal{E}_{k1}^U$ and open the respective switch $z_{ft}=0$.

3) *Step 3*: solve the resulting AC load flow problem.

This methodology could be extended to explore a larger solution space by enclosing the ad-hoc heuristic method in an outer loop and selecting lines from every $\mathcal{E}_k^U$ randomly at every iteration. Also, all permutations of switch states could be enumerated. Our result, however, lends itself well to an LNS heuristic method, which is proposed next. To restrict and control the number of STs considered in heuristic MINLP instance, we define a reduction of the previously defined UES, called reduced unique edge set (rUES).

Definition 2 (rUES) Define an rUES $\mathcal{E}_k^{U,\psi}$, such that $\mathcal{E}_k^{U,\psi}\subseteq\mathcal{E}_k^U$, $\left|\mathcal{E}_k^{U,\psi}\right|\geq 1$, and $\sum_{k=1}^{\beta(\mathcal{N})}\left|\mathcal{E}_k^{U,\psi}\right|=\psi$.

Several remarks must be made. Analogously to the UES, we call $\mathcal{E}^{U,\psi}=\{\mathcal{E}_1^{U,\psi},\mathcal{E}_2^{U,\psi},\dots,\mathcal{E}_{\beta(\mathcal{N})}^{U,\psi}\}$ the rUES. Definition 2 enforces various requirements that may seem difficult to ensure at first glance. However, this can be achieved by a simple procedure. First, add a single line to each $\mathcal{E}_i^{U,\psi}$ from the respective set $\mathcal{E}_i^U$. Then, arbitrarily or according to a rule, add lines to set $\mathcal{E}_k^{U,\psi}$, until $\sum_{k=1}^{\beta(\mathcal{N})}|\mathcal{E}_k^{U,\psi}|=\psi$. One can easily observe that all requirements hold. Given the rUES $\mathcal{E}_k^{U,\psi}$, an H-DSR$_{(13)}$ instance can be constructed as:

$$\begin{cases}\text{(1a)-(1h)}\\ \mathcal{E}^{\mathcal{S}}=\bigcup_{k=1}^{\beta(\mathcal{N})}\mathcal{E}_k^{U,\psi}\end{cases}\tag{13a}$$

$$\sum_{ft\in\mathcal{E}_k^{U,\psi}} z_{ft}=\left|\mathcal{E}_k^{U,\psi}\right|-1\quad\forall k=1,2,\dots,\beta(\mathcal{N})\tag{13b}$$

Equation (13b) enforces the removal of exactly one edge per rUES, ensuring that the resulting graph is an ST by Theorem 1. The full procedure to construct and solve H-DSR$_{(13)}$ instances is summarized as follows.

Step 1: generate a $\mathcal{B}$ of the fully connected network.

Step 2: construct all $\beta(\mathcal{N})$ UESs $\mathcal{E}_k^U$.

Step 3: construct the rUESs $\mathcal{E}_\psi^U$ for a given ψ, prioritizing edges with highest reactance x_{ft}.

Step 4: create a feasible MIP start using *Step 1* of ad-hoc heuristic method.

Step 5: formulate and solve the resulting H-DSR$_{(13)}$ instance.

A. Analysis of Problem Complexities

A corner stone to reduce complexity in the proposed heuristic method is relaxing constraints as described in Section II-B-1) with violations checked a posteriori, which yields a tighter formulation. However, H-DSR$_{(13)}$ can quickly become expensive to solve for larger systems, depending on ψ. A general analysis of DSR complexity can be found in [50]. These results are extended to include the models introduced. Let $\tau(\mathcal{N})$ denote the number of STs in $\mathcal{N}$. As the main complexity measure for these combinatorial problems, the total number of STs in $\mathcal{N}$ is used. C-DSR$_{(12)}$ and RR-DSR$_{(11)}$ consider all STs, while H-DSR$_{(13)}$ considers an adjustable subset. Additionally, we compare the number of integer variables and mixed-integer constraints, coupling these variables with each other as well as non-linear PF constraints. These also have an impact on model complexity and *ct*.

1) Complexity of C-DSR$_{(12)}$ and RR-DSR$_{(11)}$

Let $\tau^C(\mathcal{N})$ denote the number of STs that are considered by model C-DSR$_{(12)}$ given $\mathcal{N}$. As C-DSR$_{(12)}$ considers all STs, one has $\tau^C(\mathcal{N})=\tau(\mathcal{N})$. A closed form to obtain τ is known as matrix-tree theorem [51]. When it comes to the number of integer variables, the number of cycle edges must be introduced as a measure. Let $\alpha(\mathcal{N})=\left|\bigcup_i\mathcal{E}(\mathcal{C}_i^{\mathcal{N}})\right|$ denote the number of cycle edges (see Definition 7 in Supplementary Material A) in $\mathcal{N}$. How these can be determined is discussed in [39]. For RR-DSR$_{(11)}$ and C-DSR$_{(12)}$, the number of integer variables is equal to α. Regardless of the model (including H-DSR$_{(13)}$) for each discrete variable z_{ft}, four mixed-integer constraints in (1e) and (1d) are created. For RR-DSR$_{(11)}$, a single additional constraint (11b) is added, and for C-DSR$_{(12)}$, the single constraint (12c) and $\left|\mathcal{C}^{\mathcal{N}}\right|$ constraints (12b) are added, whereby it has $\left|\mathcal{C}^{\mathcal{N}}\right|$ more constraints as RR-DSR$_{(11)}$ has. For easier comparisons, $\alpha(\mathcal{N})$ is stated for every test case.

2) Complexity of H-DSR$_{(13)}$

Let $\tau^H(\mathcal{N})$ denote the number of STs that are considered by model H-DSR$_{(13)}$. $\tau^H(\mathcal{N})$ can be computed as:

$$\tau^H(\mathcal{N})=\prod_{i=1}^{\beta(\mathcal{N})}\mathcal{E}_i^{U,\psi}\tag{14}$$

The result in Theorem 1 states that exactly one line $e\in\mathcal{E}_i^{U,\psi}$ in each rUES must to be switched off to obtain an ST. In other words, a single line e must be selected from each $\mathcal{E}_i^{U,\psi}$. For a single set $\mathcal{E}_i^{U,\psi}$, there are $\left|\mathcal{E}_i^{U,\psi}\right|$ possibilities to select one element. Considering all $\mathcal{E}_i^{U,\psi}\in\mathcal{E}^{U,\psi}$, there are $\prod_{i=1}^{\beta(\mathcal{N})}\mathcal{E}_i^{U,\psi}$ possibilities to select $\beta(\mathcal{N})$ elements. In general, $\tau^H\leq\tau^C$, since an H-DSR$_{(13)}$ instance can implicitly consider at most all STs. The values of τ^H and τ^C are included alongside the results in Section IV. When it comes to the number of integer variables, an H-DSR$_{(13)}$ instance has exactly ψ. As ψ can at most reach $\alpha(\mathcal{N})$, the numbers of discrete variables and mixed-integer constraints are significantly reduced. In addition, constraint (13b) is added, ensuring acyclicity.

B. Comparison of H-DSR$_{(13)}$ and C-DSR$_{(12)}$

If the computation time allows, it is of interest to consider a maximum number of candidate STs in an H-DSR$_{(13)}$ instance. This is achieved by choosing a large value of ψ. Considering all candidate integer variables in an instance H-DSR$_{(13)}$, i. e., passing $\mathcal{E}^{U,\psi}=\mathcal{E}^U$ as input, an instance of H-DSR$_{(13)}$ and C-DSR$_{(12)}$ may be equivalent.

Corollary 1 C-DSR$_{(12)}$ and H-DSR$_{(13)}$ are equivalent, if:

$$\bigcup_{k=1}^{|\mathcal{C}^{\mathcal{N}}|}\mathcal{E}_k^{\mathcal{N}}=\bigcup_{i=1}^{\beta(\mathcal{N})}\mathcal{E}_i^{U,\psi}\left(=\bigcup_{j=1}^{\beta(\mathcal{N})}\mathcal{E}_j^{U}\right) \tag{15}$$

However, condition (15) does not commonly apply and can be read as every cycle edge exclusively belonging to a single FC. In other words, no edges must be shared by any FC, which means that all cycles in a graph are fundamental.

C. Explanation of Proposed Heuristic Method

Before the computational results are discussed, the proposed heuristic method is described in detail based on the 22-bus system displayed in Fig. 1, where a green marker indicates the substation. As described in Section III, a CB must be obtained first. The FCs obtained, i.e., $\mathcal{E}_1^{\mathcal{B}}$, $\mathcal{E}_2^{\mathcal{B}}$, $\mathcal{E}_3^{\mathcal{B}}$, and $\mathcal{E}_4^{\mathcal{B}}$, are shown in Fig. 1(a)-(d). Based on these, the sets $\mathcal{E}_k^{U}$ are created, which are shown in Fig. 1(e) in the same color as the FCs they belong to. In fact, it can be observed that $\beta(\mathcal{N})=4$ UESs are formed. Also, it can be observed that their edges indeed appear only in their respective FC and not in others. Next, as we construct the rUES for a given ψ, the sets $\mathcal{E}^{U,\psi}$ are created. An important set is $\mathcal{E}^{U,\beta(\mathcal{N})}$, where every element $\mathcal{E}_k^{U,\beta(\mathcal{N})}$ contains a single line. For the 22-bus system, the set $\mathcal{E}^{U,4}$ is illustrated in Fig. 1(f). By constraint (13a), the single line in each of $\psi=\beta(\mathcal{N})=4$ sets must be de-energized, which must result in an ST by Theorem 1 and can be visually verified. These rUESs can then be extended, until $\mathcal{E}^{U,\psi}=\mathcal{E}^{U}$, which holds when $\psi=\left|\bigcup_{i,\ldots,\beta(\mathcal{N})}\mathcal{E}_i^{U}\right|=12$ for the 22-bus system.

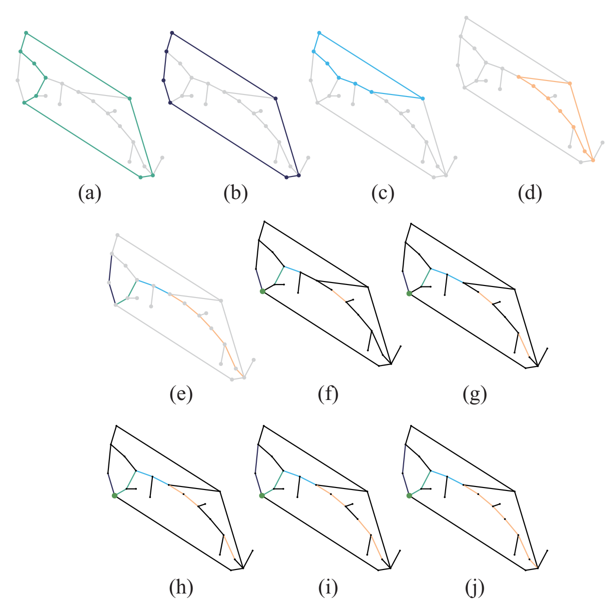

Fig. 1. FCs in a CB of 22-bus system, UESs, and rUESs. (a) $\mathcal{E}_1^{\mathcal{B}}$. (b) $\mathcal{E}_2^{\mathcal{B}}$. (c) $\mathcal{E}_3^{\mathcal{B}}$. (d) $\mathcal{E}_4^{\mathcal{B}}$. (e) $\mathcal{E}_k^{U}$. (f) $\mathcal{E}^{U,4}$. (g) $\mathcal{E}^{U,6}$. (h) $\mathcal{E}^{U,8}$. (i) $\mathcal{E}^{U,10}$. (j) $\mathcal{E}^{U,12}$

IV. Case Studies

To solve these models, the MINLP solver Juniper was used [47], with IPOPT [52] set as the NLP solver. The source code of Juniper was slightly adjusted to facilitate the logging of computational statistics to create plots. For the non-convex problems discussed, even removing integrality, Juniper is a heuristic method itself. There are no guarantees of global optimality. The term "optimal" will be used, meaning the best solution found. When mentioning the MIP gap, one must keep in mind that the lower bound computed by Juniper may not be the actual lower bound for the particular problem instance. The graph algorithms mentioned were implemented in the Julia programming language [53], relying on routines in Graphs.jl [54]. All optimization models were implemented using JuMP.jl [55] and using PowerModels.jl [44] as a reference. For our PF validation instance, the maximal difference to ACP formulation of PowerModel is smaller than 9.3×10^{-9} for any variable. All computations were performed on a laptop with an Intel i7-1165G7 clocked at 2.80 GHz and 16 GB of RAM.

A. Interpretation of Plots

1) Optimization Process

The results are visualized by plotting the incumbent objective value (an upper bound of the optimal objective value) over ct. These plots, like Fig. (2a), depict statistics for different problem instances. A diamond marker represents a new incumbent solution. Especially for larger instances, e.g., $\psi=90$, IPOPT may not converge on the NLP constructed by Juniper to check whether an MIP starts, or more generally, MIP solution is feasible. Then, the first marker appears only once the first feasible solution is found. Solid lines depict the current upper bound set by the objective value of the incumbent solution. An upper bound is not plotted before a solution is found. If no solution is found for a model, respective statistics only appear in the respective table.

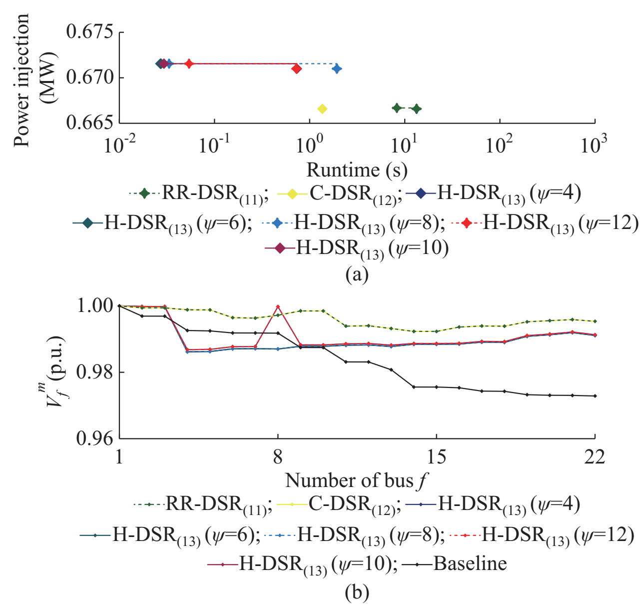

Fig. 2. Optimization process and V_f^m. (a) Optimization process. (b) V_f^m.

2) Topologies

When topologies are given in this paper, violations of constraints (2) and (3) are highlighted orange or red. If $0.05\le\left|V_f^m-v^{base}\right|<0.1$, the respective bus is colored orange. If $0.1\le\left|V_f^m-v^{base}\right|$, red is used. The same applies to lines with regard to $\bar{s}$ and $\bar{\bar{s}}$. The width of the elements is scaled with the severity of violations.

B. Optimization of an Altered 22-bus System

Due to limited size, the test case (22-bus system) considered was introduced in [56]. In total, this test case has 22 buses, 25 branch elements, and a system-wide load of 662.4 kW and 657.5 kvar, respectively. As the feeder with a base voltage of 11 kV is originally radial, adjustments were made to the system, as shown in Table I.

TABLE I
LINES ADDED TO 22-BUS SYSTEM

From bus	To bus	r (p.u.)	x (p.u.)	$\bar{s}_{ft}$ (MVA)
1	8	0.130	0.560	999
1	21	0.123	0.560	999
7	12	0.061	0.031	999
12	22	0.061	0.031	999

Lines were added, so parts of the feeder can be re-energized from opposite ends, and operating switches are feasible without immediately disconnecting the system. Based on Fig. 1(f) - (j), it can be confirmed that applying H-DSR$_{(13)}$ runs at a risk of excluding good solutions. Only a small subset of lines is switchable, as opposed to C-DSR$_{(12)}$ and RR-DSR$_{(11)}$, which has the benefit of finding good solutions faster. By examining the optimal topologies obtained for different instances in Fig. 3, it can be observed that the optimal topology identified by C-DSR$_{(12)}$ and RR-DSR$_{(11)}$ cannot be discovered by any H-DSR$_{(13)}$ instance when the latter is constructed based on the pre-determined CB. This shows that good solutions are excluded from the feasible region. Using H-DSR$_{(13)}$, losses can be reduced by 6% over the reference solution. By using C-DSR$_{(12)}$ and RR-DSR$_{(11)}$, reductions of more than 50% are possible.

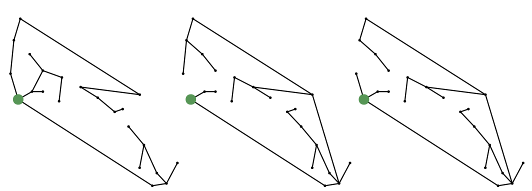

Fig. 3. Best topologies for 22-bus system. (a) H-DSR$_{(13)}$ ($\psi=4,6,8$). (b) H-DSR$_{(13)}$ ($\psi=10,12$). (c) RR-DSR$_{(11)}$/C-DSR$_{(12)}$.

For this and all the following test cases, H-DSR$_{(13)}$ with $\psi=\beta(\mathcal{N})$ serves as the reference solution. Table II contains more data on the different problem instances, and Fig. 2(a) visualizes the optimization process, but both highlight the same observation. By using H-DSR$_{(13)}$, good solutions are available and are the quickest. While C-DSR$_{(12)}$ and RR-DSR$_{(11)}$ find even better solutions, RR-DSR$_{(11)}$ requires much more *ct* than competing models. This is because the constraint (11b) only excludes subgraphs that do not have the right number of edges, yet cannot filter out topologies that meet the edge number requirement but are not STs.

TABLE II
RESULTS FOR 22-BUS SYSTEM

Method	τ^H	τ^C	p_g (MW)	p^L (kW)	Δp^L (%)	γ^v (V)	γ^s (MVA)	*ct* (s)
H-DSR ($\psi=4$)	1	1	0.672	9.153	0	0	0	0.016
H-DSR ($\psi=6$)	4	4	0.672	9.153	0	0	0	0.025
H-DSR ($\psi=8$)	12	12	0.672	9.153	0	0	0	1.343
H-DSR ($\psi=10$)	32	32	0.671	8.601	6.023	0	0	0.744
H-DSR ($\psi=12$)	48	48	0.671	8.601	6.023	0	0	0.691
C-DSR	1476	1476	0.667	4.192	54.198	0	0	1.361
RR-DSR	1476	1476	0.667	4.192	54.198	0	0	13.303

Note: $|\mathcal{E}|=25$, $\alpha(\mathcal{N})=20$, and C-DSR and RR-DSR are with no MIP start.

For the 22-bus system, $|\mathcal{E}|!/(|\mathcal{E}|-\beta(\mathcal{N}))!=303600$ subgraphs with $|\mathcal{V}|-1$ edges exist, of which only 1476 are STs according to τ^C, as shown in Table II. This confirms the results in [39].

C. Optimization of MV-rural

MV-rural is the test case with 95 buses and 100 lines that is available in the SimBench library [57]. Base voltage v^{base} is 20 kV. Statistics are reported after being converted to the MATPOWER [58] format. Conversion is done by expanding the existing converters in PandaPower to obtain a **.mat* file. The total load summed over all buses amounts to 17.26 MW and 6.82 Mvar. The total generation of RESs amounts to 25.57 MW. Two distinct scenarios are created by including and excluding RESs. MV-rural has the structure of a typical MV system in Germany that is meshed but operated in a radial manner. The total number of STs computed amounts to 5569200.

1) MV-rural Without RESs

To create a first instance of MV-rural without RESs, all generation by RESs is removed, which represents a traditional scenario of a load-dominated system. The results for MV-rural without RESs are summarized in Table III. The results of topology optimization are shown in Fig. 4, where the yellow markers represent voltage violations of the 5% voltage band. Figure 5(a) presents the optimization process, and V_f^m is shown in Fig. 5(b).

For H-DSR$_{(13)}$, good solutions can be identified extremely rapidly, and its robustness is demonstrated by the fact that all instances are solvable. While Juniper can find a strong solution for C-DSR$_{(12)}$ quickly, it times out after the 900-s limit when solving RR-DSR$_{(11)}$ without yielding any solution. H-DSR$_{(13)}$ shows significant improvements over the reference solution of up to 46.21% in reduced losses, and voltage violations of the 5% voltage band can be prevented as indicated in column γ^v of Table III.

2) MV-rural with RESs

The results for MV-rural with RESs are presented in Table IV.

TABLE III
RESULTS FOR MV-RURAL WITHOUT RESSs

Method	τ^H	τ^C	p_g (MW)	p^L (MW)	Δp^L (%)	γ^v (p.u.)	γ^s (p.u.)	ct (s)
H-DSR ($\psi=6$)	1	1	17.725	0.469	0	0.020	0	0.110
H-DSR ($\psi=16$)	288	288	17.554	0.298	36.587	0.003	0	2.207
H-DSR ($\psi=26$)	3600	3600	17.526	0.270	42.527	0	0	3.350
H-DSR ($\psi=36$)	14976	14976	17.519	0.263	43.904	0	0	4.999
H-DSR ($\psi=46$)	45696	45696	17.514	0.258	45.107	0	0	5.622
H-DSR ($\psi=66$)	489600	489600	17.509	0.253	46.211	0	0	14.148
H-DSR ($\psi=90$)	3481920	3481920	17.509	0.253	46.211	0	0	21.642
Baseline	1	1	17.623	0.367	21.742	0.009	0	0.041
C-DSR	5569200	5569200	17.510	0.250	46.210	0	0	11.820
RR-DSR	5569200	5569200	17.510	0.250	46.210	0	0	606.920

Note: $|\mathcal{E}|=100$, and $\alpha(\mathcal{N})=93$.

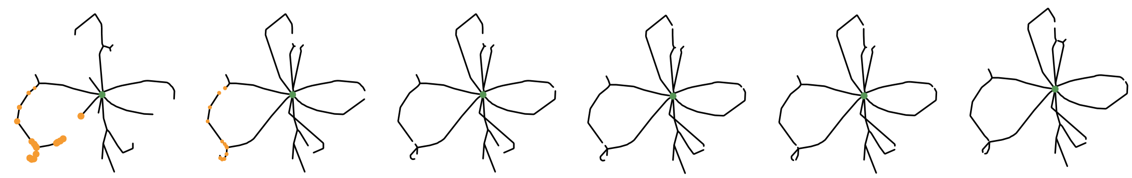

(a) (b) (c) (d) (e) (f)

Fig. 4. Results of topology optimization. (a) H-DSR$_{(13)}$ ($\psi=6$). (b) H-DSR$_{(13)}$ ($\psi=16$). (c) H-DSR$_{(13)}$ ($\psi=26$). (d) H-DSR$_{(13)}$ ($\psi=36$). (e) H-DSR$_{(13)}$ ($\psi=46$). (f) C-DSR$_{(13)}$/H-DSR$_{(13)}$ ($\psi=66, 90$).

TABLE IV
RESULTS FOR MV-RURAL WITH RESSs

Method	τ^H	τ^C	ρ (MW)	p^L (MW)	Δp^L (%)	γ^v (p.u.)	γ^s (MVA)	ct (s)
H-DSR ($\psi=6$)	1	1	−8.089	0.22	0	0	0	0.103
H-DSR ($\psi=16$)	288	288	−8.134	0.175	20.580	0	0	6.151
H-DSR ($\psi=26$)	3600	3600	−8.135	0.174	20.743	0	0	8.487
H-DSR ($\psi=36$)	14976	14976	−8.135	0.174	20.743	0	0	14.521
H-DSR ($\psi=46$)	45696	45696	−8.134	0.175	20.575	0	0	17.855
H-DSR ($\psi=66$)	489600	489600	−8.137	0.172	21.608	0	0	55.283
H-DSR ($\psi=90$)	3481920	3481920	−8.141	0.168	23.436	0	0	53.142
Baseline	1	1	−8.112	0.197	10.540	0	0	0.018
C-DSR	5569200	5569200			Does not converge to a feasible point			
C-DSR (with MIP start)	5569200	5569200	−8.177	0.131	33.910	0	0	22.870
RR-DSR	5569200	5569200						906.910

Note: $|\mathcal{E}|=100$, and $\alpha(\mathcal{N})=93$.

It can be observed that the PFs are reversed. Injection into the feeder p^G is negative, which means that net power is exported to the system. Hence, under MV-rural with RESs, more power is produced than consumed. Here, a key observation can be made regarding the models described and the applicability in RES-dominated and traditional loading scenarios. In the scenarios dominated by RESs in (8), the objective function (1a) still behaves as expected. Active power losses of the power flowing out of the feeder are minimized, maximizing the power exported. For $\psi=46$, a slightly worse solution is classified as optimal than the two previous H-DSR$_{(13)}$ instances. This is due to a sufficiently small optimality gap after additional branching. The feasibility and performance of DSR models for MV-rural with RESs are shown in Fig. 6.

D. Optimization of MV-semiurban

Larger-scale problem instances like MV-semiurban have 22 lines more than MV-rural but are much harder to solve using C-DSR$_{(12)}$. In [39], it is found that for larger systems, C-DSR$_{(12)}$ can rapidly become too difficult to be solved in a timely manner. Therefore, it is of interest how H-DSR$_{(13)}$ performs in the MV-semiurban test case. In Fig. 7, for MV-semiurban without RESs, a solution for C-DSR$_{(12)}$ is found after 600 s, and for H-DSR$_{(13)}$, strong solutions are available within seconds. For this test case, the original baseline contains a loop, for which H-DSR$_{(13)}$ would have to be extended to make a meaningful comparison. Hence, the baseline is neglected. However, H-DSR$_{(13)}$ could easily be adjusted to accommodate such cases.

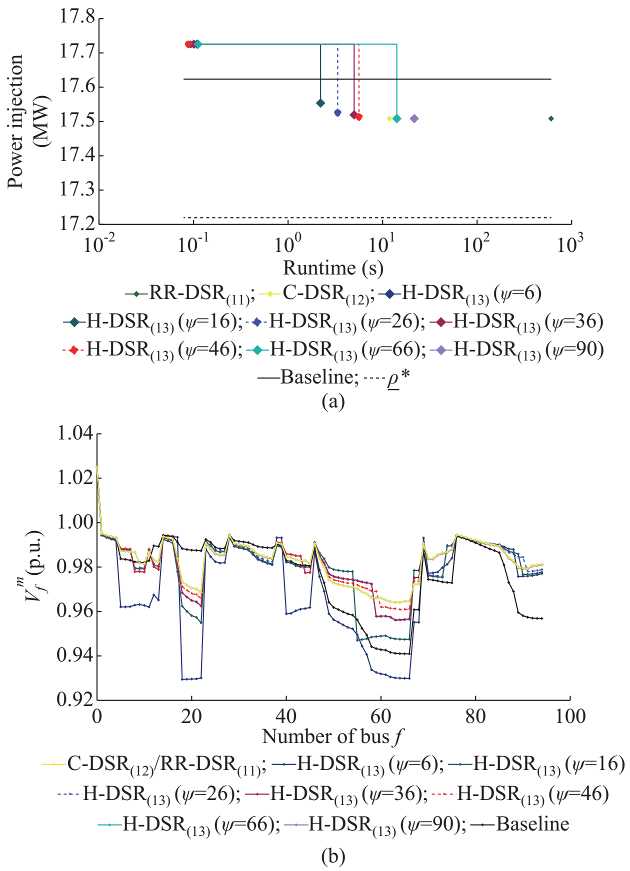

Fig. 5. Performance comparison of H-DSR$_{(13)}$, C-DSR$_{(12)}$, and RR-DSR$_{(11)}$ for MV-rural system without RESs. (a) Optimization process. (b) V_f^m.

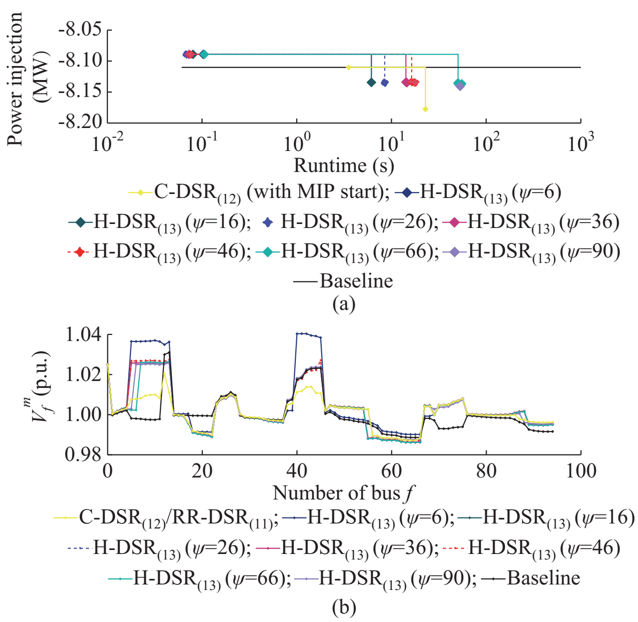

Fig. 6. Feasibility and performance of DSR models for MV-rural with RESs. (a) Optimization process. (b) V_f^m.

We reiterate that an advantage of our formulation is that exact AC PF constraints support arbitrary topological structures, unlike many approximations, which mean radial and cyclic systems and those that have both characteristics. However, edge cases are neglected in this paper to maintain focus.

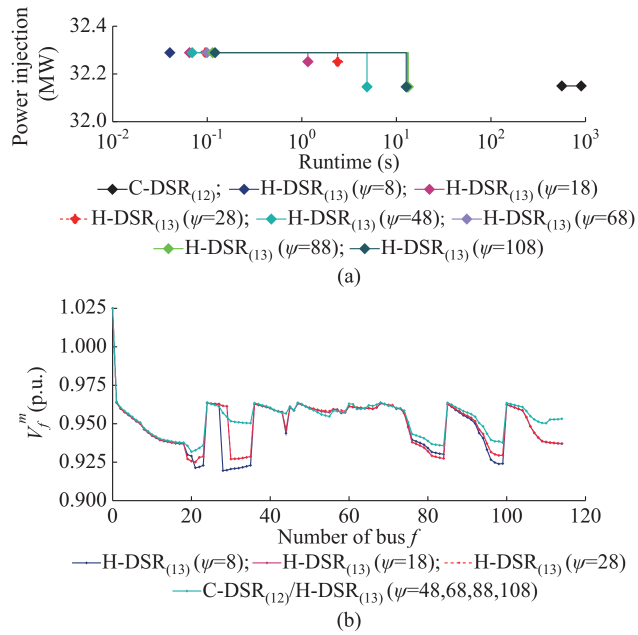

Fig. 7. Feasibility and performance of DSR models for MV-semiurban without RESs. (a) Optimization process. (b) V_f^m.

In this test case, Juniper again converges consistently solving H-DSR$_{(13)}$ instances on MV-semiurban. The results of optimized topologies for MV-semiurban DSR are shown in Fig. 8. Good solutions can be found quickly. For $\psi=48$, H-DSR$_{(13)}$ outperforms C-DSR$_{(12)}$ by two orders of magnitude in terms of *ct*, producing a better result. Table V lists the result for MV-semiurban without RESs.

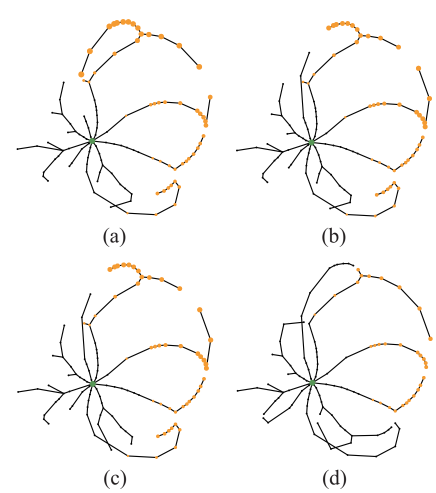

Fig. 8. Results of optimized topologies for MV-semiurban DSR. (a) H-DSR$_{(13)}$ ($\psi=8$). (b) H-DSR$_{(13)}$ ($\psi=18$). (c) H-DSR$_{(13)}$ ($\psi=28$). (d) C-DSR$_{(12)}$/H-DSR$_{(13)}$ ($\psi=48$).

V. Conclusion

This paper proposes a cycle-basis-informed heuristic method for radial DSR (H-DSR$_{(13)}$) and validates its effectiveness through extensive case studies. The results demonstrate that H-DSR$_{(13)}$ exhibits robust performance. The primary contributions of this work are threefold.

TABLE V
RESULTS FOR MV-SEMIURBAN WITHOUT RES

Method	τ^H	τ^C	ρ (MW)	p^L (MW)	Δp^L (%)	γ^v (p.u.)	γ^s (MVA)	ct (s)
H-DSR ($\psi=8$)	1	1	32.289	0.649	0	0.025	0.1	0.041
H-DSR ($\psi=18$)	120	120	32.252	0.612	5.788	0.020	0.1	1.220
H-DSR ($\psi=28$)	9000	9000	32.251	0.611	5.906	0.020	0.1	2.273
H-DSR ($\psi=48$)	462000	462000	32.146	0.506	22.037	0.011	0.1	5.153
H-DSR ($\psi=68$)	4032000	4032000	32.146	0.506	22.037	0.011	0.1	11.756
H-DSR ($\psi=88$)	4032000	4032000	32.146	0.506	22.037	0.011	0.1	13.796
H-DSR ($\psi=108$)	4032000	4032000	32.146	0.506	22.037	0.011	0.1	13.199
C-DSR	7606189536	7606189536	32.150	0.510	21.466	0.011	0.1	900.100
RR-DSR	7606189536	7606189536						902.100

Note: $|\mathcal{E}|=122$, $\alpha(\mathcal{N})=116$, and C-DSR and RR-DSR are without MIP start.

1) A theoretical result is presented, ensuring the radiality of distribution system topologies.

2) An MINLP heuristic method is devised based on the result of H-DSR$_{(13)}$ to support distributed generation and zero-injection nodes, and it does not require the full set of cycles.

3) An in-depth comparison is conducted against RR-DSR$_{(11)}$, which is a reference model that uses the connectivity-based ST definition and C-DSR$_{(12)}$ using acyclicity.

This work can be extended in several manners. First, methods may exist to predict good CB to be used in the scope of H-DSR$_{(13)}$. In addition, better indicators may exist to predict improvement when selecting lines for switching. Computationally, instead of adopting the bilevel method that checks for post-optimization of constraint violations, a constraint generation algorithm could be employed. This would involve adding new cuts to the master problem whenever constraint violations are detected. A Lagrangian relaxation or penalty method could be used to consider constraints (2) and (3) in a monolithic formulation. Lastly, testing different solvers like Bonmin [59] and Knitro [60] would provide valuable insights.

REFERENCES

[1] A. Merlin and H. Back, "Search for a minimal-loss operating spanning tree configuration in an urban power distribution system," in *Proceedings of 1975 Power Systems Computation Conference (PSCC)*, Cambridge, England, Mar. 1975, pp. 1-18.

[2] H. Glavitsch, "Switching as means of control in the power system," *International Journal of Electrical Power & Energy Systems*, vol. 7, no. 2, pp. 92-100, Mar. 1985.

[3] A. A. Mazi, B. F. Wollenberg, and M. H. Hesse, "Corrective control of power system flows by line and bus-bar switching," *IEEE Transactions on Power Systems*, vol. 1, no. 3, pp. 258-264, May 1986.

[4] W. Shao and V. Vittal, "Corrective switching algorithm for relieving overloads and voltage violations," *IEEE Transactions on Power Systems*, vol. 20, no. 4, pp. 1877-1885, Nov. 2005.

[5] European Union, Directorate-General for Research Sustainable Energy Systems. (2006, Apr.). Vision and strategy for Europe's electricity networks of the future. [Online]. Available: https://op.europa.eu/de/publication-detail/-/publication/a2ea8d86-7216-444d-8ef5-2d789fa890fc/lan - guage-en.

[6] G. Celli, F. Pilo, G. Pisano *et al*., "Meshed v.s. radial MV distribution network in presence of large amount of DG," in *Proceedings of IEEE Power Systems Conference and Exposition*, New York, USA, Aug. 2004, pp. 1357-1362.

[7] DSO Entity. (2023, Feb.). DSOs fit for 55: challenges, practices and lessons learnt on connecting renewables to the grid. [Online]. Available: https://eudsoentity.eu/publications/download/51

[8] European Parliament. (2023, May). Directive of the European parliament and of the council on energy efficiency (recast). [Online]. Available: https://data. consilium. europa. eu/doc/document/ST-7446-2023-INIT/en/pdf

[9] Stromnetz Berlin. (2024, Jan.). Grid losses tender. [Online]. Available: https://www.stromnetz.berlin/netz-nutzen/ausschreibung-netzverlustenergie/

[10] *Technische Anschlussregel Mittelspannung*, VDE Standard VDE-AR-N 4110, 2023.

[11] Stromnetz Berlin. (2019, Feb.). Technische Anforderungen für den Anschluss an das Mittelspannungsnetz Berlin. [Online]. Available: https://www. stromnetz. berlin/files/globalassets/dokumente/technischeanschlussbedingungen/ta-mittelspannung-2019/ta_mittelspannung_berlin.pdf

[12] *Electric Power Systems Voltage Ratings (60 Hz)*, ANSI Standard, 2020.

[13] R. J. Sarfi, M. M. A. Salama, and A. Y. Chikhani, "A survey of the state of the art in distribution system reconfiguration for system loss reduction," *Electric Power Systems Research*, vol. 31, no. 1, pp. 61-70, Oct. 1994.

[14] C. Xu, Z. Liao, C. Li *et al*., "Review on interpretable machine learning in smart grid," *Energies*, vol. 15, no. 12, p. 4427, Jun. 2022.

[15] J. A. Taylor, *Convex Optimization of Power Systems*. Cambridge: Cambridge University Press, May 2018.

[16] E. Ramos, A. Exposito, J. Santos *et al*., "Path-based distribution network modeling: application to reconfiguration for loss reduction," *IEEE Transactions on Power Systems*, vol. 20, no. 2, pp. 556-564, Mar. 2005.

[17] C. Qin, Y. Zeng, and J. Liu, "Searching loops in distribution systems: an MILP-based method," in *Lecture Notes in Electrical Engineering*. Singapore: Springer Nature Singapore, 2022, pp. 413-420.

[18] A. W. Bizuayehu, A. A. S. de la Nieta, J. P. S. Catalao *et al*., "Distribution system reconfiguration in economic dispatch with high wind penetration," in *Proceedings of 2015 IEEE PES General Meeting*, Denver, USA, Aug. 2015, pp. 1-5.

[19] K. Pang, C. Wang, N. D. Hatziargyriou *et al*., "Formulation of radiality constraints for optimal microgrid formation," *IEEE Transactions on Power Systems*, vol. 38, no. 6, pp. 5341-5355, Nov. 2023.

[20] Z. N. Popovic and S. D. Knezevic, "Dynamic reconfiguration of distribution networks considering hosting capacity: a risk-based approach," *IEEE Transactions on Power Systems*, vol. 38, no. 4, pp. 3440-3450, Jul. 2022.

[21] A. Arif, S. Ma, Z. Wang *et al*., "Optimizing service restoration in distribution systems with uncertain repair time and demand," *IEEE Transactions on Power Systems*, vol. 33, no. 4, pp. 6828-6838, Nov. 2018.

[22] A. Arif, S. Ma, and Z. Wang, "Dynamic reconfiguration and fault isolation for a self-healing distribution system," in *Proceedings of 2018 IEEE/PES Transmission and Distribution Conference and Exposition* (*T&D*), Denver, USA, Feb. 2018, pp. 1-5.

[23] N. G. Paterakis, A. Mazza, S. F. Santos *et al*., "Multi-objective reconfiguration of radial distribution systems using reliability indices," *IEEE Transactions on Power Systems*, vol. 31, no. 2, pp. 1048-1062, Mar. 2016.

[24] A. Borghetti, "A mixed-integer linear programming approach for the computation of the minimum-losses radial configuration of electrical distribution networks," *IEEE Transactions on Power Systems*, vol. 27, no. 5, pp. 1264-1273, Sept. 2012.

[25] F. Capitanescu and I. Bilibin, "A tractable two-step MILP-QCP approach to on-line thermal constraint management in large radial active distribution systems," *Electric Power System Research*, vol. 140, pp. 580-587, Nov. 2016.

[26] E. Romero-Ramos, J. Riquelme-Santos, and J. Reyes, "A simpler and exact mathematical model for the computation of the minimal power losses tree," *Electric Power Systems Research*, vol. 80, pp. 562-571, May 2010.

[27] N. C. Koutsoukis, D. O. Siagkas, P. S. Georgilakis *et al*., "Online reconfiguration of active distribution networks for maximum integration of distributed generation," *IEEE Transactions on Automation Science and Engineering*, vol. 14, no. 3, pp. 437-448, May 2017.

[28] J. Jose and A. Kowli, "Path-based distribution feeder reconfiguration for optimization of losses and reliability," *IEEE Systems Journal*, vol. 14, no. 3, pp. 1417-1426, Mar. 2020.

[29] R. A. Jabr, R. Singh, and B. C. Pal, "Minimum loss network reconfiguration using mixed-integer convex programming," *IEEE Transactions on Power Systems*, vol. 27, no. 3, pp. 1106-1115, May 2012.

[30] M. Mahdavi, H. H. Alhelou, N. D. Hatziargyriou *et al*., "An efficient mathematical model for distribution system reconfiguration using AMPL," *IEEE Access*, vol. 9, pp. 79961-79993, Sept. 2021.

[31] M. Mahdavi, K. E. K. Schmitt, M. Chamana *et al*., "Evaluation of voltage fluctuations effect on reconfiguration of distribution systems," *IEEE Systems Journal*, vol. 18, pp. 198-209, Mar. 2024.

[32] M. R. Dorostkar-Ghamsari, M. Fotuhi-Firuzabad, M. Lehtonen *et al*., "Value of distribution network reconfiguration in presence of renewable energy resources," *IEEE Transactions on Power Systems*, vol. 31, no. 3, pp. 1879-1888, May 2016.

[33] Q. Peng, Y. Tang, and S. Low, "Feeder reconfiguration in distribution networks based on convex relaxation of OPF," *IEEE Transactions on Power Systems*, vol. 30, no. 4, pp. 1793-1804, Jul. 2015.

[34] K. Masteri and B. Venkatesh, "Real-time smart distribution system reconfiguration using complementarity," *Electric Power System Research*, vol. 134, pp. 97-104, May 2016.

[35] G. Raju and P. R. Bijwe, "An efficient algorithm for minimum loss reconfiguration of distribution system based on sensitivity and heuristics," *IEEE Transactions on Power Systems*, vol. 23, no. 4, pp. 1280-1287, Jul. 2008.

[36] A. De Bonis, J. P. S. Catalao, A. Mazza *et al*., "A novel optimization algorithm solving network reconfiguration," in *Proceedings of 2014 Power Systems Computation Conference*, Wrocław, Poland, Aug. 2014, pp. 1-7.

[37] M. Lavorato, J. F. Franco, M. J. Rider *et al*., "Imposing radiality constraints in distribution system optimization problems," *IEEE Transactions on Power Systems*, vol. 27, no. 1, pp. 172-180, Jan. 2012.

[38] F. Capitanescu, L. F. Ochoa, H. Margossian *et al*., "Assessing the potential of network reconfiguration to improve distributed generation hosting capacity in active distribution systems," *IEEE Transactions on Power Systems*, vol. 30, no. 1, pp. 346-356, Jan. 2015.

[39] A. Hinneck, M. Duckheim, M. Metzger *et al*. (2025, Jun.). On loss-minimal radial topologies in MV systems. [Online]. Available: https://arxiv.org/abs/2506.03422

[40] M. C. O. Borges, J. F. Franco, and M. J. Rider, "Optimal reconfiguration of electrical distribution systems using mathematical programming," *Journal of Control*, *Automation and Electrical Systems*, vol. 25, no. 1, pp. 103-111, Feb. 2014.

[41] J. Gorka and L. Roald, "Efficient representations of radiality constraints in optimization of islanding and de-energization in distribution grids," *Electric Power Systems Research*, vol. 213, p. 108578, Jun. 2022.

[42] E. Danna, E. Rothberg, and C. L. Pape, "Exploring relaxation induced neighborhoods to improve MIP solutions," *Mathematical Programming*, vol. 102, pp. 71-90, Jun. 2005.

[43] T. Bertold, "Heuristic algorithms in global MINLP solvers," Ph.D. dissertation, Technische Universitat, Berlin, Germany, 2014.

[44] C. Coffrin, R. Bent, K. Sundar *et al*., "Power models. JL: an open-source framework for exploring power flow formulations," in *Proceedings of 2018 Power Systems Computation Conference (PSCC)*, Dublin, Ireland, Jun. 2018, pp. 1-8.

[45] A. Hinneck and D. Pozo, "Optimal transmission switching: improving solver performance using heuristics," *IEEE Transactions on Power Systems*, vol. 38, no. 4, pp. 3317-3330, Apr. 2023.

[46] J. Grainger and W. Stevenson, *Power System Analysis*. New York: McGraw-Hill Professional, Jan. 1994.

[47] O. Kröger, C. Coffrin, H. Hijazi *et al*., "Juniper: an open-source nonlinear branch-and-bound solver in Julia," in *Integration of Constraint Programming, Artificial Intelligence*, *and Operations Research*, New York: Springer International Publishing, 2018, pp. 377-386.

[48] M. Lavorato, J. F. Franco, M. J. Rider *et al*., "Closure to discussion on imposing radiality constraints in distribution system optimization problems," *IEEE Transactions on Power Systems*, vol. 28, no. 2, pp. 568-569, Mar. 2013.

[49] N. E. Gibbs, "A cycle generation algorithm for finite undirected linear graphs," *Journal of ACM*, vol. 16, pp. 564-568, Oct. 1969.

[50] L. H. Macedo, J. F. Franco, M. Mahdavi *et al*., "A contribution to the optimization of the reconfiguration problem in radial distribution systems," *Journal of Control, Automation and Electrical Systems*, vol. 29, pp. 756-768, Dec. 2018.

[51] W. Kocay and D. L. Kreher, "Graphs, algorithms, and optimization," in *Discrete Mathematics and Its Applications*. London: CRC Press, 2023.

[52] A. Wächter and L. T. Biegler, "On the implementation of an interior-point filter line-search algorithm for large-scale nonlinear programming," *Mathematical Programming*, vol. 106, pp. 25-57, Mar. 2006.

[53] J. Bezanson, A. Edelman, S. Karpinski *et al*., "Julia: a fresh approach to numerical computing," *SIAM Review*, vol. 59, no. 1, pp. 65-98, Jan. 2017.

[54] J. Fairbanks, M. Besanon, S. Schlly *et al*. (2021, Nov.). Juliagraphs//graphs.jl: an optimized graphs package for the julia programming language. [Online]. Available: https://github.com/JuliaGraphs/Graphs.jl/

[55] M. Lubin, O. Dowson, J. D. Garcia *et al*., "JuMP 1.0: recent improvements to a modeling language for mathematical optimization," *Mathematical Programming Computation*, vol. 15, no. 3, pp. 581-589, Mar. 2023.

[56] M. R. Raju, K. R. Murthy, and K. Ravindra, "Direct search algorithm for capacitive compensation in radial distribution systems," *International Journal of Electrical Power & Energy Systems*, vol. 42, no. 1, pp. 24-30, Jan. 2012.

[57] S. Meinecke, D. Sarajli, S. R. Drauz *et al*., "Simbench-a benchmark dataset of electric power systems to compare innovative solutions based on power flow analysis," *Energies*, vol. 13, p. 3290, Jun. 2020.

[58] R. D. Zimmerman, C. E. Murillo-Snchez, and R. J. Thomas, "Matpower: steady-state operations, planning, and analyss tools for power systems research and education," *IEEE Transactions on Power Systems*, vol. 26, no. 1, pp. 12-19, Jan. 2011.

[59] P. Bonami, L. T. Biegler, A. R. Conn *et al*., "An algorithmic framework for convex mixed integer nonlinear programs," *Discrete Optimization*, vol. 5, pp. 186-204, May 2008.

[60] R. H. Byrd, J. Nocedal, and R. A. Waltz, "Knitro: an integrated package for nonlinear optimization," in *Nonconvex Optimization and Its Applications*, Boston: Springer US, 2006, pp. 35-59.

Anton Hinneck received the B.Sc. and M.Sc. degrees in industrial engineering at the Berlin Institute of Technology, Berlin, Germany, in 2015 and 2018, respectively. He is currently pursuing the Ph.D. degree at the Faculty of Electrical Engineering and Information Technology, Technical University of Darmstadt, Darmstadt, Germany. He also works as an Engineer at Distribution System Operator Stromnetz, Berlin, Germany. His research interests include optimization method for energy system operation and planning.

Mathias Duckheim received the Ph. D. degree in theoretical physics from the University of Basel, Basel, Switzerland. He is a Principal Expert in the Sustainable Energy & Infrastructure Team at Siemens AG, Foundational Technologies, Erlangen, Germany. His research interests include modeling, operation, and automation of power grids and energy networks with high share of distributed energy resources.

Michael Metzger received the Diploma degree in mathematics and computer science at the Technical University Munich, Munich, Germany, and the Ph.D. degree in electrical engineering at the Friedrich Alexander University Erlangen-Nuermberg, Erlangen, Germany. He is the Distinguished Engineer in the Sustainable Energy & Infrastructure Team at Siemens AG, Foundational Technologies, Munich, Germany. He is also the Lecturer at the School of Engineering and Design, Technical University of Munich, Munich, Germany. His research interests include grid control, energy automation, and energy management system dealing with high share of distributed energy resources.

Stefan Niessen is a Professor with the Faculty of Electrical Engineering and Information Technology, Technical University of Darmstadt, Darmstadt, Germany, and he is also with Siemens AG, Foundational Technologies, Erlangen, Germany. He heads the Sustainable Energy & Infrastructure Team at Siemens AG. His research interests include coupling between electricity, heating, cooling, traction energy, sweet water, and chemical form of energy to improve costs, sustainability and to harvest flexibility.